The Institute of Space and Astronautical Science
Report SP No.14, December 2000

ISO Continuum Observations of Quasars at z =1–4

By

Shinki OYABU[*], Kimiaki KAWARA[*], Yumihiko TSUZUKI[*],
Yoshiaki SOFUE[*], Yasunori SATO[*], Haruyuki OKUDA[†],
Yoshiaki TANIGUCHI[‡], Hiroshi SHIBAI[§], Carlos GABRIEL[¶],
Takashi HASEGAWA[‖] and Eiji NISHIHARA[‖]

(November 1, 2000)

Abstract: Eight luminous quasars with $-30 < M_{\rm B} < -27$ at $z = 1.4$ - 3.7 have been observed in the mid- and far-infrared with ISO. To obtain spectral energy distributions (SEDs) from the UV to far-infrared, additional optical and near-infrared observations were made from the ground. The observed SEDs are compared with the mean-SED of low-redshift quasars with less luminosity ($-27 < M_{\rm B} < -22$) given by Elvis et al. (1994). There is no evidence of excess in the mid- and far-infrared in our quasar sample.

1. INTRODUCTION

IRAS was the first instrument that was sensitive enough to detect many bright quasars in the far-infrared. Neugebauer et al. (1986) have presented IRAS measurements of 179 quasars from 12 to 100 μm. Combining IRAS observations with data taken in other wavelengths, Sanders et al. (1989) have compiled SEDs from $\sim$ 0.3 nm to 6 cm of 109 quasars from the Palomar-Green (PG) survey (Green, Schmidt, & Liebert 1986). Compiling Einstein, IUE, and IRAS data supplemented with ground-based observations, Elvis et al. (1994) have presented SEDs for a sample of 47 normal quasars, and derived the mean-SEDs for radio-quiet and radio-loud quasars.

The sensitivity of IRAS was not sufficient to observe high-redshift quasars with normal luminosity, and accordingly only a few quasars at $z > 3$ with exceptionally high luminosity

[*] Institute of Astronomy, the University of Tokyo, 2-21-1 Osawa, Mitaka, Tokyo 181–0015, Japan; shinki@mtk.ioa.s.u-tokyo.ac.jp
[†] Institute of Space and Astronautical Science (ISAS), 3-1-1 Yoshinodai, Sagamihara, Kanagawa, 229-8510, Japan
[‡] Astronomical Institute, Tohoku University, Aoba, Sendai 980-8578, Japan
[§] Department of Astrophysics, School of Science, Nagoya University, Furo-cho, Chikusa-ku, Nagoya 464-8602, Japan
[¶] ISO Data Centre, Astrophysics Division of ESA, Villafranca, 28080 Madrid, Spain
[‖] Gunma Astronomical Observatory, 6860-86 Nakayama, Takayama, Agatsuma, Gunma 371-0702, Japan

have been detected in the far-infrared (Neugebauer et al. 1986; Bechtold et al. 1994; Irwin et al. 1998); F08279+5255 (APM 08279+5255) at $z = 3.87$, 2126-158 (PKS 2126-15) at $z = 3.275$, and 0320-388 at $z = 3.12$. The rest-frame far-infrared emission of high-redshift quasars can also be accessible in the millimeter and submillimeter. Up to date, more than several quasars at $z > 3$ have been detected in the region from 350 μm to 1.25 mm (e.g. Omont et al. 1996; Cimatti et al. 1998; Hughes, Dunlop, & Rawlings 1997; Benford et al. 1999).

The gross shape of SEDs is characterized by two major features; the big blue bump shortward of 0.3 μm and the infrared bump between 2 μm and 1 mm. It is generally considered that the blue bump is dominated by thermal emission from an accretion disk, where the infrared bump is made up of reradiation from dust. Many authors tried to explain the distribution of dust from the infrared bump. Sanders et al. (1989) made the infrared bump model of reradiation from dust in a distorted disk extending from 0.1 kpc to more than 1 kpc, which is heated directly by radiation from central source. Rowan-Robinson (1995) gave the model which introduces dust cloud in the narrow line region as the absorber of the central source and a starburst component contributing to the emission at 30−100 μm. The third hypothesis by Andreani, Franceschini, & Granato (1999) suggests that the infrared bump is emitted by the torus of dust which surrounds the central nuclei and reaches an equilibrium temperature which is a function of the distance from central sources and of the dimensions and chemical composition of the assumed grain components. These interpretations imply that far-infrared emission can probe the dust in circumnuclear or host galaxies, which is an important constituent in star-forming environment. Hence, the far-infrared observation of high-redshift quasars would tell the history of star-formation activity in the past.

In hoping to detect more quasars, several groups have carried out mid- and far-infrared photometry using the Infrared Space Observatory (ISO; Kessler et al. 1996). The first report of the ISO European Central Quasar Programme observing 70 quasars between 4.8 and 200 μm including high-redshift quasars has been published by Haas, Chini, & Kreysa (1998), and the ISO/NASA AGN Key Project has also observed 72 quasars and AGNs covering a range of redshift up to 4.7 (Wilkes et al. 1999). As an ISO open time program, we have undertaken the mid- and far-infrared observations of eight quasars at $1.4 < z < 3.7$ using the raster mapping mode. This paper presents the results of photometry of these quasars supplemented with optical and near-infrared data taken on the ground. Throughout this paper, $H_0 = 75 \mathrm{km\,s^{-1}\,Mpc^{-1}}$ with $q_0 = 0$ is assumed.

2. OBSERVATIONS AND RESULTS

Eight quasars have been observed with ISO to study the mid- and far-infrared properties of high-redshift quasars. To expand the wavelength coverage of SEDs from the UV to far-infrared, optical and near-infrared imaging have been undertaken.

2.1 The Sample

Table 1 lists the sample of eight quasars ordered by the sequence of ISO revolutions. The sample consists of luminous quasars with $M_\mathrm{B} <$ -28 except PC 1548+4637 and PC 1640+4628; these two quasars that were observed at the beginning of this work, turned out to be too faint to be detected in the far-infrared emission, and thus the sample selection criterion was changed to observe very luminous quasars in low far-infrared background of cirrus emission. Figure 1 presents the eight quasars (large filled diamonds) on the $z - M_\mathrm{B}$ plane together with those

Table 1: QSOs Sample

Object	R.A. (J2000)	Dec.	z	M_B[a]	Radio[b]	Rev (UT)[c]
PC 1548+4637	15:50:07.6	+46:28:55	3.544	−27.0	Quiet	169 (960504)
PC 1640+4628	16:42:05.1	+46:22:27	3.700	−26.8	Quiet	185 (960520)
H 0055-2659	00:57:58.3	−26:43:14	3.662	−29.2	Optical	380 (961130)
UM 669	01:05:16.8	−18:46:42	3.037	−28.4	Optical	415 (970104)
B 1422+231	14:24:38.1	+22:56:01	3.62	−29.8[d]	Loud	424 (970113)
PG 1630+377	16:32:01.1	+37:37:49	1.478	−28.2	Quiet	424 (970113)[e]
PG 1715+535	17:16:35.4	+53:28:15	1.940	−28.5	Quiet	712 (971027)
UM 678	02:51:40.4	−22:00:27	3.205	−29.4	Optical	781 (980104)

[a] The absolute B magnitude for $H_0 = 75 \mathrm{km\,s^{-1}\,Mpc^{-1}}$ with $q_0 = 0.0$.

[b] Radio property; Quiet = radio quiet, Loud = radio loud, and Optical = optically selected.

[c] UT is given in the yymmdd format where yy = year, mm = month, and dd = day.

[d] $M_B \sim -26$ after demagnification (see discussion).

[e] Also observed on rev. 778 (980101)

(small filled circles) in the sample by Elvis et al. (1994) and those (faint gray points) complied by Véron-Cetty & Véron (1998). All the sample quasars are radio-quiet or optically selected except B 1422+231 which is a core-dominant flat-spectrum radio source.

2.2 Mid- and Far-Infrared Data Taken with ISO

The mid-infrared observations were performed with ISOCAM (Cesarsky et al. 1996). Three broad band filters, namely, LW2 (reference wavelength 6.7 μm), LW3 (14.3 μm), and LW10 (12.0 μm) were used. All the quasars were observed in LW2 with additional measurements in LW3 or LW10. To detect faint sources against the intense background dominated by zodiacal light, the Astronomical Observation Template (AOT) CAM01 that is the micro-scan raster mapping mode was used to achieve accurate flat-fielding (e.g. Taniguchi et al. 1997; Altieri et al. 1999).

The far-infrared observations were made with ISOPHOT (Lemke et al. 1996). All the quasars were observed in the broad C_160 (170 μm) band with additional measurement in C_90 (90 μm). ISO far-infrared surveys (Kawara et al. 1998; Puget et al. 1999) clearly indicate the sky seen in the far-infrared has a clumpy structure that is made up of IR cirrus and extragalactic sources. We used the PHT22 staring raster map mode for the small maps centered on the quasar.

The standard ISO reduction software, CIA 3.0[1] and PIA 7.3[2] (Gabriel, Acosta-Pulido, & Kinkel 1997) , were used to produce ISO images by reducing the edited raw data created via the off-line processing version 7.0. Aperture photometry was then performed using IRAF[3],

[1] CIA is distributed by the ISO Data Centre and the ISOCAM Data Centre at Saclay, France.
[2] PIA is a joint development by the ESA Astrophysics Division and the ISOPHOT consortium.
[3] IRAF is distributed by NOAO.

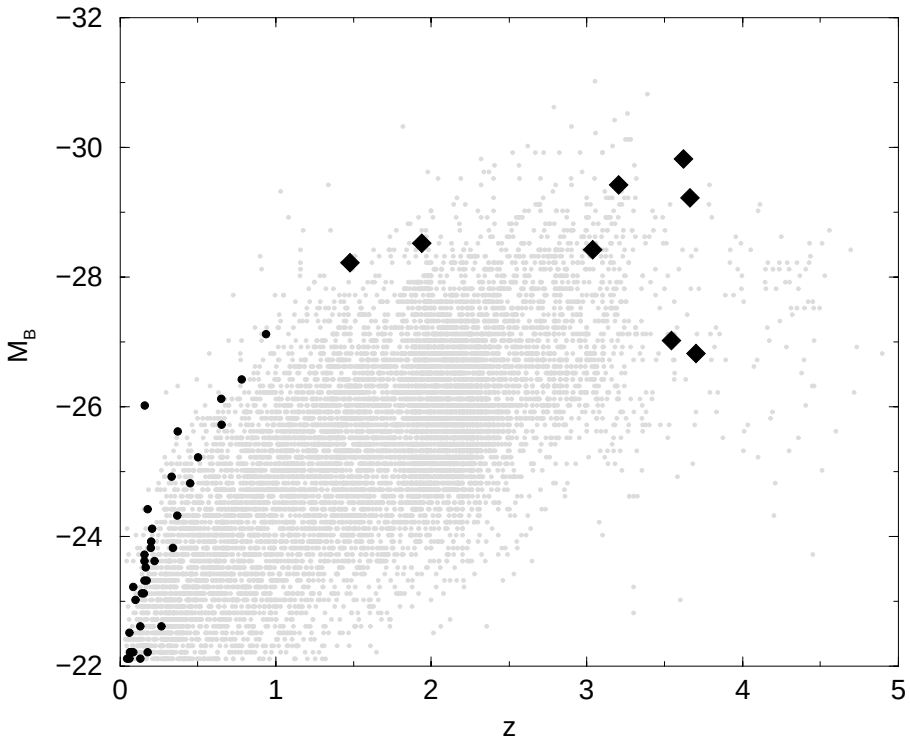

Fig. 1: Sample quasars (large filled diamonds) compared with other samples of quasars on the z - $M_{\rm B}$ plane. Small filled circles shows quasars studied by Elvis et al. (1994). Quasars cataloged by Véron-Cetty & Véron (1998) were plotted by dots, which looks like gray background on this plane.

Skyview[4] and IDL. The aperture photometry was corrected for loss of flux in the point spread function (PSF) wings by computing the same PSF model (Oyabu et al. 2000).

The results are given in Table 2 with statistical errors. PG1630+377 was observed twice at C_160 to check the variability. The uncertainty of the absolute photometric calibrations of ISO data is estimated to be 30 % (Blommaert & Cesarsky 1998; Klaas et al. 1998).

2.3 Optical and Near-Infrared Data from Ground-Based Observations

Optical images were taken on the 0.9-m telescopes at CTIO and the Schmidt 1.05-m telescope at the Kiso Observatory. Near-infrared imaging was made in the standard dithering mode on the 1.88-m telescope at the Okayama Astrophysical Observatory, NAOJ.

All the ground-based observations were performed within 24 months from the ISO observations to reduce the probability of flux variations between ISO and ground-based observations. Optical and near-infrared photometry data also supplement optical magnitudes taken by Richards et al. (1997) and Schneider, Schmidt, & Gunn (1994). All the supplementary quasars but PG 1548+4637 were observed within 27 months before the ISO observations.

[4] Skyview is distributed by IPAC.

Table 2: ISO mid/far-infrared flux densities and UV to IR luminosities

	ISOCAM(mJy)			ISOPHOT(mJy)	
Object	LW2	LW3	LW10	C_90	C_160
PC 1548+4632	0.16 ± 0.04	...	0.67 ± 0.17	8.2 ± 28	32 ± 80
PC 1640+4628	0.15 ± 0.04	...	0.29 ± 0.11	-8.3 ± 20	83 ± 121
H 0055-2659	0.29 ± 0.06	...	...	16 ± 19	-2.7 ± 60
UM 669	0.50 ± 0.01	...	...	...	-9.9 ± 18
B 1422+231	5.8 ± 0.06	15.1 ± 0.07	...	...	83 ± 56
PG 1630+377	4.3 ± 0.04	7.3 ± 0.07	...	...	5.6 ± 14^a
PG 1715+535	4.7 ± 0.06	10.3 ± 0.06	...	...	-13 ± 16
UM 678	0.73 ± 0.01	1.9 ± 0.03	...	...	-15 ± 58

[a] $f_\nu(C\_160) = 89 \pm 78$ mJy was obtained in the second observation.

3. DISCUSSION

All the quasars have been detected in the mid-infrared, while no detection above the 3 σ level has been made in the far-infrared. Figure 2 compares the restframe SEDs (L_ν;L_ν is defined by $4\pi D_{\rm L}^2 \nu f_\nu$ where $D_{\rm L}$ denotes the luminosity distance to the object.) of our quasars with the mean-SED of low-redshift quasars. This mean-SED derived by Elvis et al. (1994) and normalized at 1.25 μm, is particularly convenient for comparison with our data, because it displays the 1 σ deviation (strictly speaking 68 Kaplan-Meier percentile) envelopes. The mean-SED was normalized to the ISO LW2 ($\sim 6.7\mu$m) flux density; in many cases, LW2 ($\sim 6.7\mu$m) in the observing frame is approximately 1.25μm in the restframe. There is no evidence of far-infrared excess in the present sample.

In case of B 1422+231, however, the flux deficiency in the far-infrared may be a natural consequence of gravitational lensing. The optical and radio fluxes directly emitted from the central source are magnified by a factor of 15-30 (Patnaik et al. 1992; Hogg & Blandford 1994; Kormann, Schneider, & Bartelmann 1994). If the far-infrared emission is made up of reradiation from dust in a disk extending on kpc scales as suggested by Sanders et al. (1989), the magnification in the far-infrared will be much smaller than that in the other wavelengths where radiation comes from the central source and its vicinity (Eisenhardt et al. 1996).

Figure 3 shows the maps of C_160 for the brightest quasars B 1422+231 and PG 1715+535, which should be at the center of maps. The far-infrared detection with ISO are severely limited by the confusion due to galaxies and local peaks of the IR cirrus (Kawara et al. 1998; Herbstmeier et al. 1998). Far-infrared studies of high-redshift quasars with normal luminosity definitely require higher spatial resolutions that should be achieved by the future missions such as ASTRO-F, SIRTF, FIRST and HII/L2.

ACKNOWLEDGEMENT

We wish to thank the staff of Vilspa, CTIO, OAO, and the Kiso observatory for their assistance and hospitality. We are grateful to T. Tsuji for his continuous support to this work.

REFERENCES

Altieri, B. et al. 1999, A&A, 343, L65
Andreani, P., Franceschini, A., & Granato, G. 1999, MNRAS, 306, 161
Bechtold, J. el al. 1994, AJ, 108, 374
Benford, D. J. et al. 1999, ApJ, 518, L65
Blommaert, J. & Cesarsky, D. 1998, ISOCAM Calibration Accuracies Document (http://www.iso.vilspa.esa.es/)
Cesarsky, C. J. et al. 1996, A&A, 315, L32
Cimatti, A. et al. 1998, A&A, 329, 399
Eisenhardt, P. R. et al. 1996, ApJ, 461, 72
Elvis, M. et al. 1994, ApJS, 95, 1
Gabriel, C. et al., 1997, in: Astronomical Data Analysis Software and System VI, ed. G. Hugg & H. E. Payne (SC: ASP), 108
Green, R. F., Schmidt, M., & Liebert, J. 1986, ApJS, 61, 305
Haas, M., Chini, R., & Kreysa, E. 1998, ApJ, 503, L109
Herbstmeier, U. et al. 1998, A&A, 332, 739
Hogg, D. W. & Blandford, R. D. 1994, MNRAS, 268, 889
Hughes, D. H., Dunlop, J. S., & Rawlings, S. 1997, MNRAS, 289, 766
Irwin, M. J. et al. 1998, ApJ, 505, 529
Kawara, K. et al. 1998, A&A, 336, L9
Kessler, M. et al. 1996, A&A, 315, L27
Klaas, U. et al. 1998, ISOPHOT Calibration Accuracies (http://www.iso.vilspa.esa.es/)
Kormann, R., Schneider, P., & Bartelmann, M. 1994, A&A, 286, 357
Lemke, D. et al. 1996, A&A, 315, L64
Neugebauer, G. et al. 1986, ApJ, 308, 815
Omont, A. et al. 1996, A&A, 315, 1
Oyabu, S. et al. 2000, A&A, in press (astro-ph/0010550)
Patnaik, A. R. et al. 1992, MNRAS, 259, 1
Puget, J. L. et al. 1999, A&A, 345, 29
Richards, G. T. et al. 1997, PASP, 109, 39
Rowan-Robinson, M. 1995, MNRAS, 272, 737
Sanders, D. B. et al. 1989, ApJ, 347, 29
Schneider, D. P., Schmidt, M., & Gunn, J. E. 1994, AJ, 107, 1245
Taniguchi Y. et al. 1997, A&A, 328, L9
Véron-Cetty, M. P. & Véron P. 1998, ESO Scientific Report No. 18, A Catalogue of Quasars and Active Galactic Nuclei 8th Edition (Garching: ESO)
Wilkes, B. et al. 1999, in: The Universe as Seen by ISO, ed. M. Kessler (Noordwijk: ESA), 845

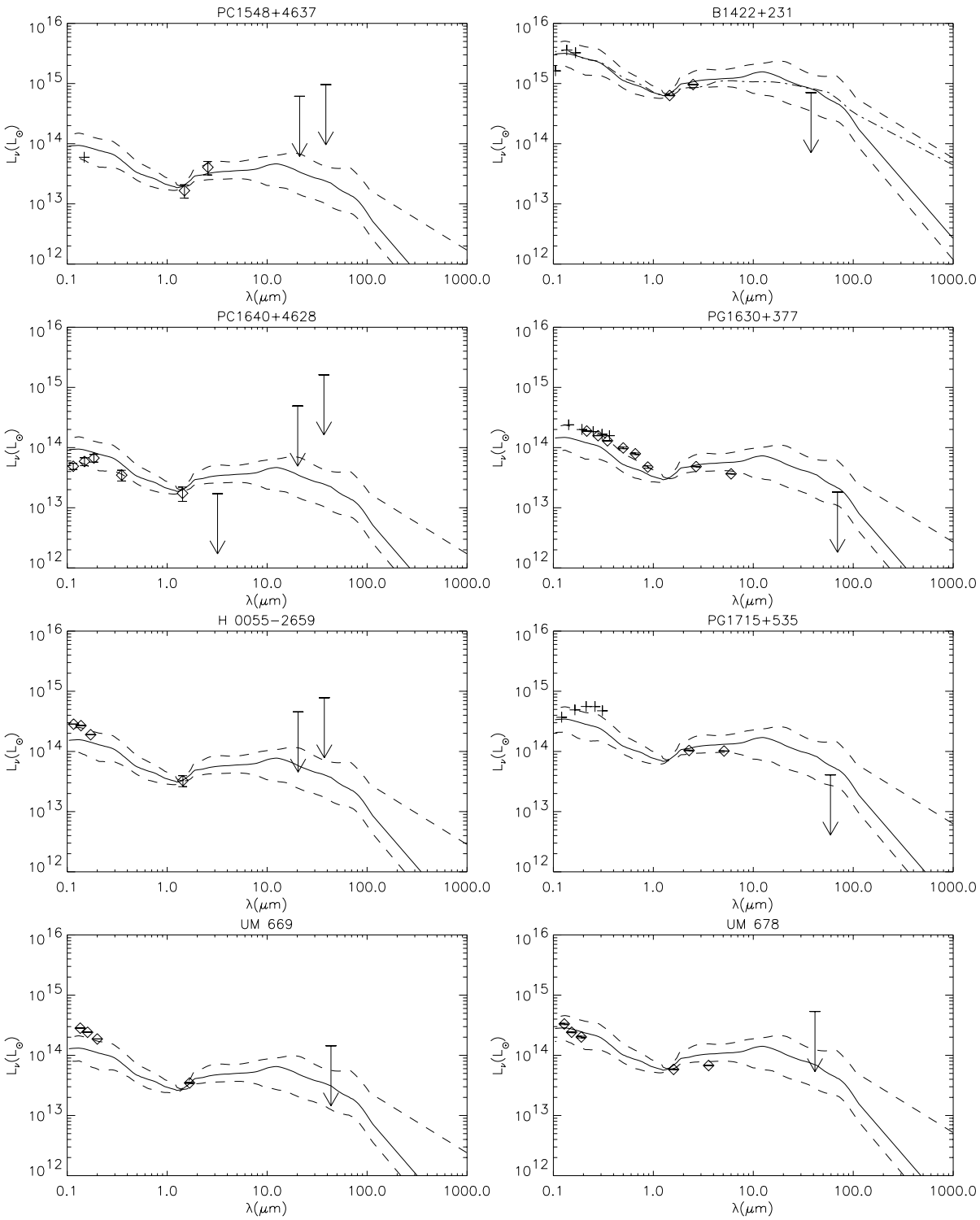

Fig. 2: Restframe SEDs compared with the mean-SED of low-redshift quasars compiled by Elvis et al. (1994). Dashed lines show the 1 σ deviation (actually 68 Kaplan-Meier percentile) envelopes. Asterisks denote data taken by Richards et al. (1997) and Schneider et al. (1994). The dot-dashed line for B1422+231 shows the mean-SED of radio-loud quasars from Elvis et al. (1994).

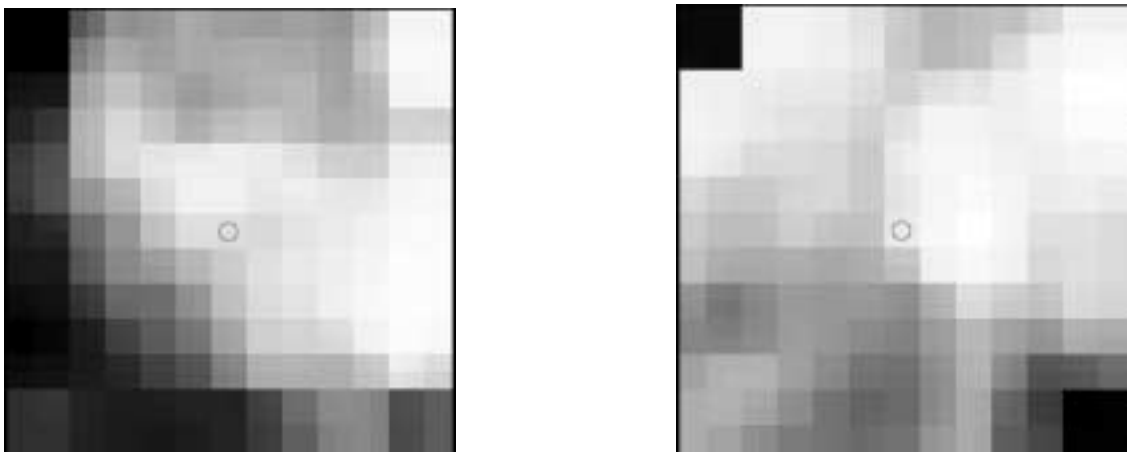

Fig. 3: Sample of C_160 far-infrared images: (Left) B 1422+231 (Right) PG 1715+535. Quasars should be located in the center of images, where small circles are marked. The brighter is higher intensities.